Free Radical Research

ISSN: 1071-5762 (Print) 1029-2470 (Online) Journal homepage: http://www.tandfonline.com/loi/ifra20

LC/MS analysis of cardiolipins in substantia nigra and plasma of rotenone-treated rats: Implication for mitochondrial dysfunction in Parkinson's disease

Y. Y. Tyurina, A. M. Polimova, E. Maciel, V. A. Tyurin, V. I. Kapralova, D. E. Winnica, A. S. Vikulina, M. R. M. Domingues, J. McCoy, L. H. Sanders, H. Bayır, J. T. Greenamyre & V. E. Kagan

To cite this article: Y. Y. Tyurina, A. M. Polimova, E. Maciel, V. A. Tyurin, V. I. Kapralova, D. E. Winnica, A. S. Vikulina, M. R. M. Domingues, J. McCoy, L. H. Sanders, H. Bayır, J. T. Greenamyre & V. E. Kagan (2015) LC/MS analysis of cardiolipins in substantia nigra and plasma of rotenone-treated rats: Implication for mitochondrial dysfunction in Parkinson's disease, Free Radical Research, 49:5, 681-691, DOI: 10.3109/10715762.2015.1005085

To link to this article: http://dx.doi.org/10.3109/10715762.2015.1005085

Free Radical Research, May 2015; 49(5): 681–691

ISSN 1071-5762 print/ISSN 1029-2470 online
DOI: 10.3109/10715762.2015.1005085

informa
healthcare

ORIGINAL ARTICLE

LC/MS analysis of cardiolipins in substantia nigra and plasma of rotenone-treated rats: Implication for mitochondrial dysfunction in Parkinson's disease

Y. Y. Tyurina[1,2], A. M. Polimova[1,2,7], E. Maciel[5,6], V. A. Tyurin[1,2], V. I. Kapralova[1,2], D. E. Winnica[1,2], A. S. Vikulina[1,2,7], M. R. M. Domingues[5,6], J. McCoy[3], L. H. Sanders[3], H. Bayır[1,2,4], J. T. Greenamyre[3] & V. E. Kagan[1,2]

[1]*Center for Free Radical and Antioxidant Health, University of Pittsburgh, Pittsburgh, USA,* [2]*Departments of Environmental and Occupational Health, University of Pittsburgh, Pittsburgh, USA,* [3]*Department of Neurology, University of Pittsburgh, Pittsburgh, USA,* [4]*Department of Critical Care Medicine, University of Pittsburgh, Pittsburgh, USA,* [5]*Mass Spectrometry Center, University of Aveiro, Aveiro, Portugal,* [6]*Department of Chemistry, QOPNA, University of Aveiro, Aveiro, Portugal, and* [7]*Department of Medical Biophysics, Faculty of Fundamental Medicine, MV Lomonosov Moscow State University, Moscow, Russia*

Abstract

Exposure to rotenone *in vivo* results in selective degeneration of dopaminergic neurons and development of neuropathologic features of Parkinson's disease (PD). As rotenone acts as an inhibitor of mitochondrial respiratory complex I, we employed oxidative lipidomics to assess oxidative metabolism of a mitochondria-specific phospholipid, cardiolipin (CL), in substantia nigra (SN) of exposed animals. We found a significant reduction in oxidizable polyunsaturated fatty acid (PUFA)-containing CL molecular species. We further revealed increased contents of mono-oxygenated CL species at late stages of the exposure. Notably, linoleic acid in *sn*-1 position was the major oxidation substrate yielding its mono-hydroxy- and epoxy-derivatives whereas more readily "oxidizable" fatty acid residues (arachidonic and docosahexaenoic acids) remained non-oxidized. Elevated levels of PUFA CLs were detected in plasma of rats exposed to rotenone. Characterization of oxidatively modified CL molecular species in SN and detection of PUFA-containing CL species in plasma may contribute to better understanding of the PD pathogenesis and lead to the development of new biomarkers of mitochondrial dysfunction associated with this disease.

Keywords: Parkinson's disease, cardiolipin, oxygenated cardiolipin species, oxygenated linoleic acid

Introduction

Parkinson's disease (PD) is a neurodegenerative disorder in the elderly characterized by the loss of dopaminergic neurons in substantia nigra (SN) [1]. Mitochondrial dysfunction and oxidative stress are believed to be important contributors to the neuronal loss and the pathogenesis of PD [2–6]. Decreased activity of mitochondrial complex I [7], reduced amounts of glutathione [8], protein modification [9], DNA damage [10] and lipid oxidation [11] have been documented in the SN compacta of patients with PD in many studies. While polyunsaturated phospholipids are the major substrates for oxidative modifications [12], evaluation of lipid peroxidation products has been restricted to detection of secondary oxidation products such as 4-hydroxy-2-nonenal [13,14] and essential information on molecular targets, particularly specific polyunsaturated molecular species of phospholipids undergoing oxidation and leading to mitochondrial dysfunction and their association with PD, is lacking.

Given that oxidation products formed from polyunsaturated molecular species of a mitochondria-specific phospholipid, cardiolipin (CL) have been identified as important cell death signals [12,15], their systematic analysis in PD-relevant samples may be particularly important. However, reliable identification and quantitation of these products even using sensitive contemporary liquid chromatography/mass spectrometry (LC/MS) protocols is challenging due to the inherent instability, fast metabolic conversions, as well as high diversification of oxidized species resulting in their low steady-state concentrations [16]. We have developed several advanced techniques of oxidative lipidomics that allowed physical separation of oxidized and non-oxidized phospholipids as well as accurate identification and quantitative analysis of oxygenated molecular species of phospholipids using LC or high-performance thin-layer chromatography (HPTLC) protocols [17–19] along with different versions of MS combined with enzymatic hydrolysis of fatty acid residues from modified phospholipids [20]. Here, using a rat rotenone model of PD [21] and oxidative lipidomics approach we were able, for the first time, to identify and quantitatively characterize oxygenated molecular species of CL formed in dysfunctional mitochondria in SN as well as in CL in plasma.

Correspondence: Yulia Y. Tyurina, PhD, Center for Free Radical and Antioxidant Health, Department of Environmental and Occupational Health, University of Pittsburgh, Bridgeside Point, 100 Technology Drive, Suite 350, Pittsburgh, PA, 15219. USA. Tel: +412-383-5099. Fax: +412-624-9361. E-mail: yyt1@pitt.edu

(Received date: 16 October 2014; Accepted date: 5 January 2015; Published online: 4 March 2015)

Methods

Rat rotenone model

The Institutional Animal Care and Use Committee of the University of Pittsburgh approved all experiments utilizing animals. Male Lewis rats (7–9 months old, Charles River) were injected intraperitoneally with vehicle or 3.0 mg/kg/day of rotenone (Sigma-Aldrich) either once, for five daily injections or treated to parkinsonian endpoint. We chose to evaluate one and five daily injection paradigms because we have previously detected mitochondrial DNA damage in the SN and peripheral tissues following rotenone treatment at these time points [22,23]. Animals treated with rotenone to parkinsonian endpoint recapitulate many of the key pathological features of PD [24,25]. Animals treated with rotenone to parkinsonian endpoint (10–14 days) were sacrificed when animals displayed behavioral features including bradykinesia, postural instability/gait disturbances, and rigidity. Rat brains were first removed from the skull and rinsed in cold 1X phosphate-buffered saline to remove any surface blood. Brains were placed on a cold Petri dish and cut in half into the right and left hemisphere. Using a blade and forceps precise micro-dissection of the ventral midbrain was performed and the tissue was flash frozen in liquid nitrogen and stored at − 80°C.

Extraction of lipids

Lipids were extracted from SN and plasma using the Folch and Bligh–Dyer procedures, respectively [26,27]. Lipid phosphorus was determined by a micro-method [28].

Analysis of esterified fatty acids

To release esterified fatty acids, total lipids were treated with either phospholipase A_1 (PLA_1) from *Thermomyces lanuginosus* (10 μl/μmol of phospholipids) (Sigma-Aldrich, St. Louis, MO, USA) or phospholipase A_2 (PLA_2) from porcine pancreas (10 U/μmol of phospholipids) (Sigma-Aldrich, St. Louis, MO, USA) in 0.5 M borate buffer, pH: 9.0 containing 20 mM cholic acid, 2 mM $CaCl_2$ and 100 μM diethylenetriaminepentaacetic acid (DTPA) for 60 min at 37°C. Under these conditions, almost 99% of phospholipids were hydrolyzed. Liberated oxygenated and non-oxygenated fatty acids were separated from lipids and lysolipids by solid-phase extraction using phospholipid removal plates (Phenomenex, Torrance, CA, USA) and analyzed by LC/MS as described [29]. Briefly, LC/MS in negative mode was performed using a Dionex Ultimate™ 3000 high-performance liquid chromatography (HPLC) coupled online to a Q-Exactive hybrid quadrupole-orbitrap mass spectrometer (Thermo Fisher Scientific, San Jose, CA, USA). Fatty acids were separated on a reverse-phase column (C_{18} Luna, 3 μm, 150 × 2 mm, Phenomenex, Torrance, CA, USA) with flow rate 0.2 mL/min using gradient solvents containing 5 mM ammonium acetate [A: tetrahydrofuran/methanol/water/CH_3COOH, 25:30:50:0.1 (v/v/v/v) and B: methanol/water 90:10 (v/v)]. The column was eluted for the first 3 min isocratically at 50% B, from 3 to 23 min with a linear gradient from 50% solvent B to 98% solvent B, then 23–40 min isocratically using 98% solvent B, 40–42 min with a linear gradient from 98% solvent B to 50% solvent B, and 42–60 min isocratically using 50% solvent B for equilibration of the column. Standards of oxygenated fatty acids were purchased from Cayman Chemical Co. (Ann Arbor, MI, USA).

Analysis of CL

LC/MS was performed as previously described [29]. Briefly, LC/MS in negative mode was performed using a Dionex UltiMate™ 3000 HPLC coupled online to a linear ion-trap mass spectrometer (LXQ, Thermo Fisher Scientific, San Jose, CA, USA). Thus, m/z values for CL molecular species were presented to 1 decimal place. Total lipids were separated on a normal-phase column [Silica Luna 3 μm, 100A, 150 × 2 mm, (Phenomenex, Torrance CA)] with flow rate of 0.2 mL/min using gradient solvents containing 5 mM CH_3COONH_4 [A—n-hexane:2-propanol:water, 43:57:1 (v/v/v) and B—n-hexane:2-propanol:water, 43:57:10 (v/v/v)]. Tetra-myristoyl CL (TMCL) (Avanti polar lipids, Alabaster, AL, USA) was used as an internal MS standard.

Analysis of oxygenated CL

CL was separated by two-dimensional (2D) HPTLC [30], and CL and oxygenated CL were analyzed by LC/MS as described [18]. To prevent lipid oxidation during separation, chromatography was performed under N_2 conditions on DTPA-treated silica plates (5 × 5 cm, Whatman). LC/MS in negative mode was performed using a Dionex UltiMate™ 3000 RSLCnano System coupled online with Q-Exactive hybrid quadrupole-orbitrap mass spectrometer (Thermo Fisher Scientific, San Jose, CA, USA) using a C_8 column (Luna 3 μm, 100 Å, 150 × 2 mm, Phenomenex, Torrance, CA, USA) with flow rate of 0.15 mL/min using an isocratic solvent system consisting of 2-propanol:water: triethylamine:acetic acid, 45:5:0.25:0.25, v/v. The resolution was set up at 140000 which corresponds to 5 ppm in m/z measurement error. Thus, m/z values for CLs and their oxidation species were presented to 4 decimal places. TMCL (Avanti polar lipids, Alabaster, AL, USA) was used as an internal MS standard. TMCL molecular species is not usually present in the brain (and other tissues) and does not interfere with the endogenous CLs and widely used as an internal standard [31]. The ionization efficiencies of individual molecular species of CLs, particularly of those with differing fatty acid chains, may be different. To minimize the potential inaccuracies, the tuning of mass spectrometers was performed using Tetra-linoleoyl-cardiolipin (TLCL), (C18:2)4-CL. In addition, TLCL was also utilized as a reference standard to build calibration curves employed for quantitative assessments of CLs in the brain. Finally, we were able to compare the total amounts of CLs in SN samples based on LC/MS analysis and summation of individual

molecular species with that obtained from the direct determinations after 2D-HPTLC separation of total phospholipid extracts. These comparisons showed good coincidence of the CL amounts determined in two independent ways.

Statistics

The results are presented as mean ± standard deviation (SD) values from at least three experiments, and statistical analyses were performed by either paired/unpaired Student's t-test or one-way analysis of variance. The statistical significance of differences was set at $p < 0.05$.

Results

Rotenone is a highly lipophilic compound that can cross the blood–brain barrier [32,33]. Its toxicity mechanisms are mostly associated with the binding to and inhibiting electron transport at the level of complex I and generation of superoxide radicals [15,34,35]. These mitochondria-related effects lead to selective degeneration of dopaminergic neurons and produce neuropathologic features of PD [21]. Therefore, our oxidative lipidomic efforts to detect mitochondria-specific modification of lipids were focused on the analysis of CLs in SN of rats exposed to rotenone. The flow chart representing our analytical approach is shown in Figure 1.

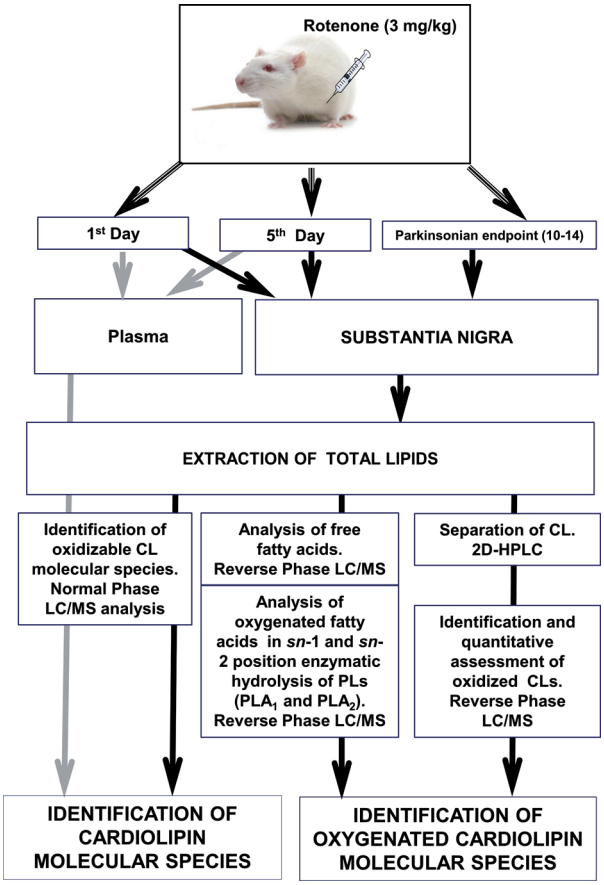

Figure 1. Flowchart representing analytical approach to assess CL and its oxygenated species in plasma and SN.

Because of high diversification of oxidatively modified phospholipids with potentially low content of each of them, we chose to simplify the analytical task by reducing the number of oxygenated molecular species. To this end, we treated the total lipid extracts with either PLA_1 or PLA_2 to release fatty acid residues from *sn*-1 and *sn*-2 positions of phospholipids, respectively. This allowed the detection of oxidation products in a limited number of molecular species of oxidizable polyunsaturated fatty acids (PUFAs). PUFAs were mainly represented by linoleic ($C_{18:2}$), arachidonic ($C_{20:4}$), and docosahexaenoic ($C_{22:6}$) acids and predominantly localized in *sn*-2 position (Figure 2). Surprisingly, while the content of PUFA in *sn*-1 position was significantly lower than that in *sn*-2, oxygenated fatty acid species were released almost exclusively upon PLA_1 treatment (Figure 3). Furthermore, among the PUFAs released, linoleic acid ($C_{18:2,}$ with 2 double bonds) underwent oxidative modification to mono-hydroxy (HODE) and epoxy (EpOME) derivatives (Figure 3), whereas more polyunsaturated, hence more readily "oxidizable" fatty acid residues such as $C_{20:4}$, and $C_{22:6}$, remained non-oxidized. A substantial increase in epoxy-molecular species of $C_{18:2}$ was detected at day 5 and

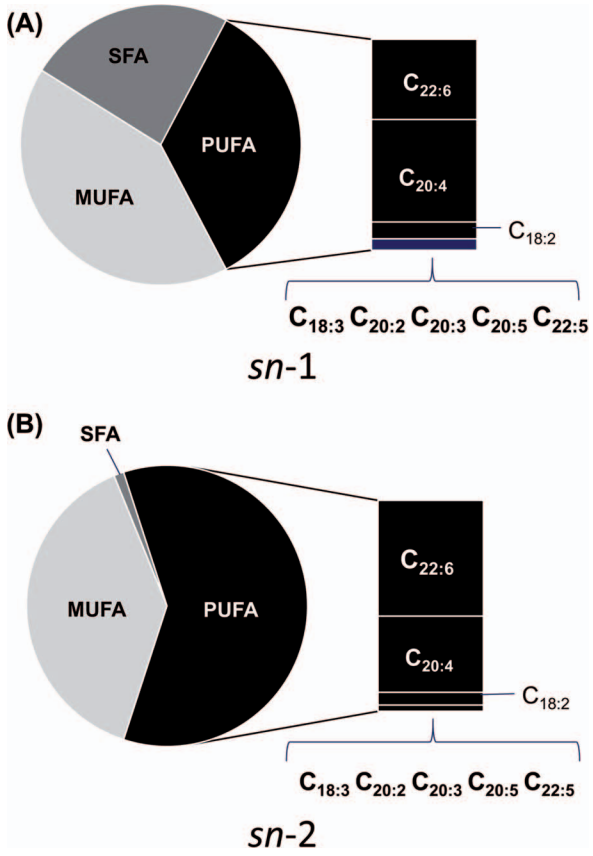

Figure 2. Profile of fatty acids liberated from total phospholipids extracted from SN by either PLA_1 (A, *sn*-1 position) or PLA_2 (B, *sn*-2 position). SFA: saturated fatty acids, MUFA: monounsaturated fatty acid, PUFA: polyunsaturated fatty acid; $C_{18:2}$: octadecadienoic acid (linoleic acid); $C_{18:3}$: octadecatrienoic acid, $C_{20:2}$: eicosadienoic acid, $C_{20:3}$: eicosatrienoic acid, $C_{20:4}$: eicosatetraenoic acid (arachidonic acid), $C_{20:5}$: eicosapentaenoic acid, $C_{22:5}$: docosapentaenoic acid, $C_{22:6}$: docosahexaenoic acid.

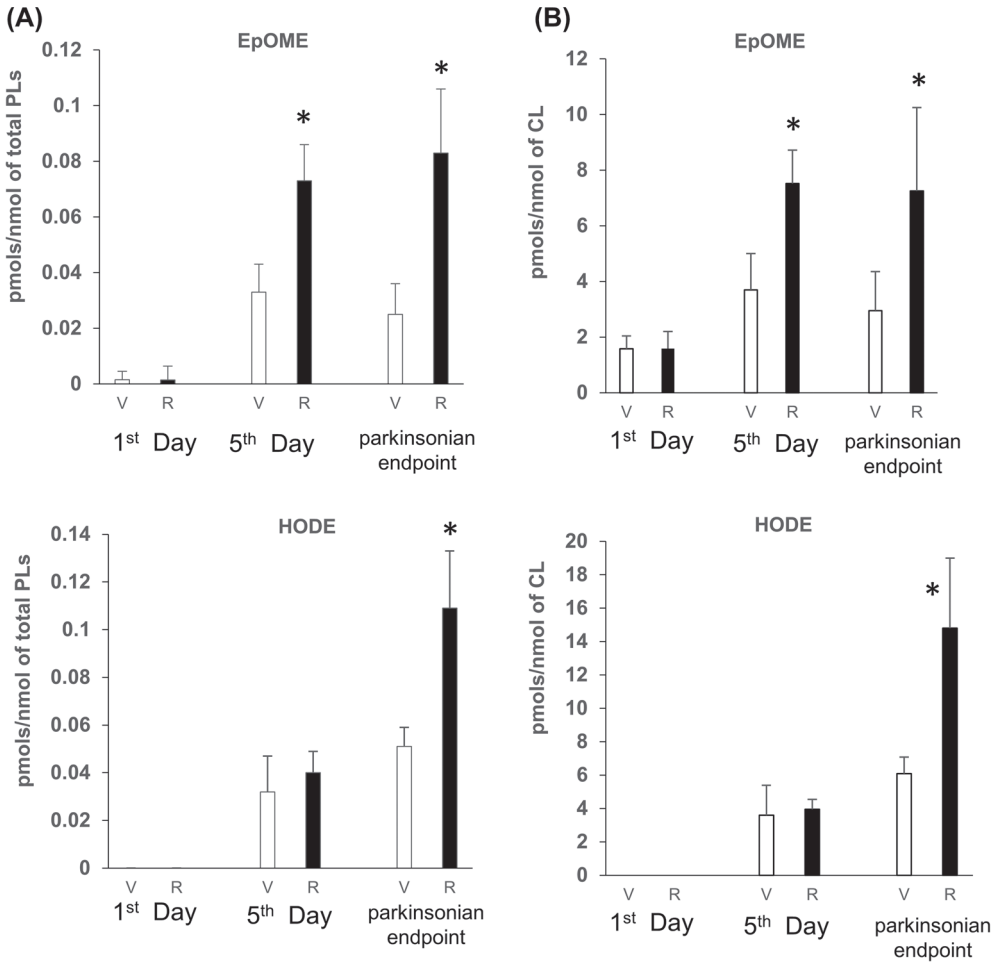

Figure 3. Quantitative assessment of oxygenated $C_{18:2}$ (octadecadienoic acid) liberated by PLA_1 from SN total phospholipids. HODE: hydroxy species of $C_{18:2}$, EpOME: epoxy species of $C_{18:2}$. Released oxygenated fatty acids were analyzed by reverse-phase LC/MS after solid-phase extraction. Data are normalized (A) per nmol of total phospholipids (PLs) and (B) per nmol of CL.

parkinsonian endpoint (Figure 3); however, the changes in the content of hydroxy species of $C_{18:2}$ were significant only at parkinsonian endpoint. No accumulation of oxygenated $C_{18:2}$ was observed at day 1 of exposure (Figure 3). No oxygenated PUFAs were detected in samples obtained from rats exposed to rotenone and treated with PLA_2 (data not shown). In major classes of phospholipids including phosphatidylcholine, phosphatidylethanolamine, and phosphatidylserine, oxidizable PUFAs ($C_{18:2}$, $C_{20:4}$ and $C_{22:6}$) occupy predominantly the *sn*-2 position whereas in CL they can be equally distributed between *sn*-1 and *sn*-2 positions [18]. This suggests that oxygenated esterified $C_{18:2}$ detected in SN of rotenone-treated rats likely originated from the *sn*-1 position of CL.

Therefore, we further specifically focused on the analysis of CLs in SN. Using normal-phase LC followed by full MS and MS^2 analysis, we identified oxidizable CL molecular species containing fatty acids with 2–6 double bonds (Table I, Figure 4A, B). Quantitative assessments revealed a substantial reduction of these species in SN of rotenone-exposed rats at all time points studied compared with control animals (Figure 4C). Notably, all these polyunsaturated CL species contained at least one $C_{18:2}$ residue. No changes in the CL content from cortex of the same rats were detected (data not shown). Therefore, we suggested that decrease in the content of oxidizable CL was linked to rotenone-induced damage of mitochondria in SN.

Assuming that lipid peroxidation can contribute to the depletion of oxidizable CL we further characterized oxygenated CL species in SN. CLs were pre-separated by HPTLC and subjected to reverse-phase LC to resolve non-oxidized versus oxidized CL species after which high mass accuracy MS was employed to identify CL oxygenated species (Figure 5). We detected significantly increased content of mono-oxygenated CL species at parkinsonian endpoint (Figure 6). Quantitative analysis revealed accumulation of several mono-oxygenated CL species (m/z: 1443.9903, 1446.0038, 1472.0189, 1491.9891, 1494.0033, 1515.9889, and 1518.0026) (Figure 6) which originated from oxidizable CL species (m/z: 1427.9966, 1430.0077, 1456.0260, 1475.9943, 1478.0067, 1499.9929, and 1502.0061). Notably, all of these species were reduced by rotenone exposure and contained at least one $C_{18:2}$ residue (Table I, Figure 3). No accumulation of oxygenated CL in SN on day 1 was detected (data not shown).

Assuming that mitochondria with their CLs and oxidized CLs can be released from damaged cells into extracellular environments and act as damage-associated

Table I. Major CL and CL oxidized species detected in SN and plasma from rats exposed to rotenone.

m/z	CN:DB	CL molecular species	Mono-oxygenated CL species in SN (m/z)	CL species detected in plasma (m/z)
1425.9771	70:5	16:1/18:1/18:1/**18:2** 16:0/**18:2**/18:1/**18:2**	1441.9735	1425.9832
1427.9966	70:4	16:0/18:1/18:1/**18:2** 16:1/18:1/18:1/18:1 16:0/**18:2**/18:1/18:1	1443.9903	1427.9962
1430.0077	70:3	16:0/**18:2**/18:1/18:0 16:0/18:1/18:1/18:1 16:1/18:1/18:1/18:0	1446.0038	1430.0088
1454.0059	72:5	18:1/18:1/18:1/**18:2**	1470.0074	1454.0051
1456.0260	72:4	18:1/18:1/18:0/**18:2**	1472.0189	1456.0249
1475.9943	74:8	18:1/18:1/**18:2**/20:4 18:0/**18:2**/**18:2**/20:4	1491.9891	1475.9922
1478.0067	74:7	18:0/18:1/**18:2**/20:4 18;1/18:1/18:1/20:4 18:1/**18:2**/18:0/20:4 16:0/18:1/**18:2**/22:4 16:1/18:0/**18:2**/22:4 16:0/18:1/18:0/22:6 16:1/18:0/18:0/22:6	1494.0033	1478.0150
1499.9929	76:10	18:1/20:4/18:1/20:4 **18:2**/18:0/**18:2**/22:6 18:1/18:1/**18:2**/22:6	1515.9889	ND
1502.0061	76:9	18:1/**18:2**/18:0/22:6 18:0/**18:2**/18:1/22:6 18:1/18:1/18:1/22:6 18:1/20:2/18:0/20:4 **18:2**/20:3/18:0/20:4 18:1/20:3/18:1/20:4	1518.0026	ND

CL, cardiolipin; CN and DB refer to the total carbon atoms in the fatty acid chains and total number of double bonds, respectively; ND, not detected

molecular patterns [36], we performed analysis of CL in plasma of rats at two time points (day 1 and day 5) after the exposure to rotenone. MS analysis revealed the increase of relative intensity for CL molecular species with m/z: 1425.9832, 1427.9962, 1430.0088, 1454.0051, 1456.0249, 1475.9922, and 1478.0150 (Figure 7). Relative intensities for several individual CL molecular species as well as their total content were significantly higher on days 1 and 5 compared with those for the corresponding controls (Figure 7B, C). All CLs in plasma were represented by non-oxygenated molecular species. The sensitivity of LC/MS assay for oxygenated CL is approximately 10 nM. Given that the observed levels of oxygenated CL in rotenone-treated rats constituted only 0.2% of its total content in the brain, the expected increased levels in plasma would be on the order of 0.3 nM. Assuming that metabolic conversions of oxygenated CL (e.g., by lipoprotein-associated Lp-PLA_2 [18]) would result in its hydrolysis, the contents of oxygenated CL would be even lower.

Discussion

Oxidatively modified phospholipids have been recognized as important signals in acute injury and chronic diseases [37–39]. CL is a negatively charged phospholipid with four fatty acid residues [40]. In normal conditions, CL is found exclusively in the inner-mitochondrial membrane where it accounts for 25% of all phospholipids [41] and essential for normal functions of many proteins, including the activity of respiratory complexes [42–45]. Accumulation of oxygenated CL molecular species and their hydrolysis products has been demonstrated for acute brain injury caused by trauma and cardiac arrest [46,47], hyperoxic- and nanoparticle-induced lung injury [48,49], as well as acute irradiation syndrome [18,29,50]. Polyunsaturated CLs in the brain have been considered not only as oxidation substrates [12] but also as a source of oxygenated lipid mediators [18,46,51].

Rotenone—a known inhibitor of complex I in mitochondria—has been used to mimic clinical features of PD [1]. The rotenone model is characterized by slow and progressive loss of dopaminergic neurons and formation of Lewy bodies in SN [1]. Degeneration of dopaminergic neurons in SN has been long associated with mitochondrial dysfunction. Given that disrupted electron transport may be linked to the enhanced reactive oxygen species production in mitochondria [52], we sought to test whether this would result in oxidative modifications of a susceptible phospholipid target, CL, that is highly concentrated in close proximity to complex I in the inner mitochondrial membrane [53,54]. Using the rat rotenone model of PD, here, we demonstrate, for the first time, the accumulation of CL oxygenated species in SN.

Two major pathways triggered in dysfunctional mitochondria—mitophagy and apoptosis—may be involved

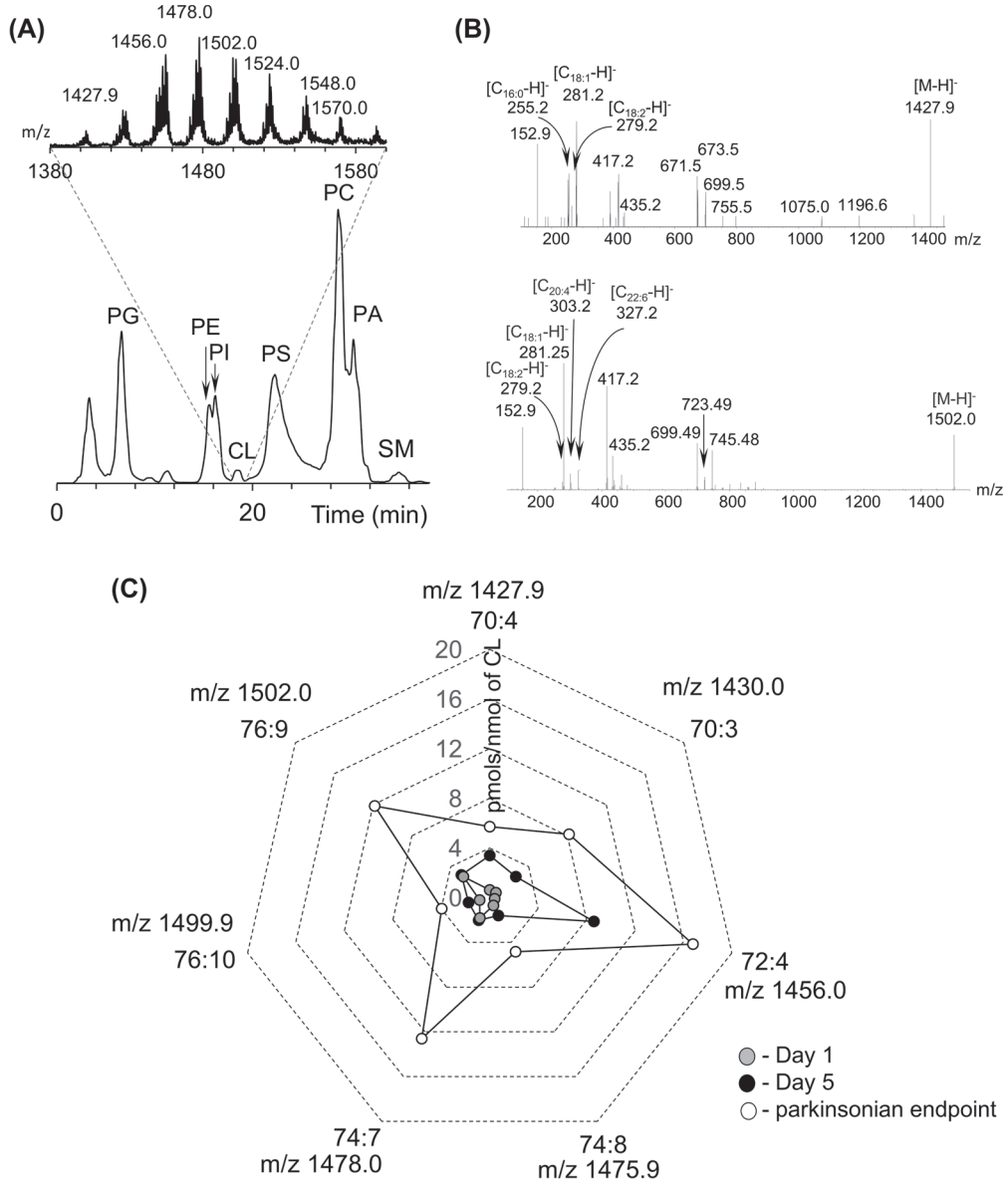

Figure 4. Assessment of CL in SN by normal-phase LC/MS. (A) Typical normal-phase LC/MS chromatogram of phospholipids and full mass spectrum of CL (insert) extracted from SN obtained from control rats. Data were acquired in negative mode. CL: cardiolipin, PA: phosphatidic acid, PC: phosphatidylcholine, PE: phosphatidylethanolamine, PG: phosphatidylglycerol, PI: phosphatidylinositol, PS: phosphatidylserine, SM: sphingomyelin. (B) MS^2 fragmentation of CL molecular ions with m/z 1427.9 (upper panel) and m/z 1502.0 (lower panel). (C) Quantitative assessments of CL in SN of rotenone-exposed rats. The data are presented as rotenone-induced decreases in the amounts of oxidizable CL molecular species.

in responses of dopaminergic neurons to rotenone in SN [55–57]. For both pathways CLs have been recognized as signaling molecules [16,58]. In the case of pro-survival mitophagy CL is externalized to the outer leaflet of the outer mitochondrial membrane but does not undergo oxidation [58]. The externalized CL acts as a signal recognized by LC3 to facilitate the elimination of damaged mitochondria and rescue the cell [58]. In contrast, accumulation of oxygenated CL species has been identified as an early event in the execution of apoptotic program [15] resulting in the release of cytochrome c into the cytosol and activation of caspases and cell death [15]. Our oxidative lipidomic protocols revealed the early loss of oxidizable linoleic-acid-containing CL species (on days 1 and 5 after exposure to rotenone) and accumulation of CL oxidation products in the same molecular species in SN on the parkinsonian endpoint. Of note, in this model animals received rotenone daily, thus the total dose of rotenone was increasing during the exposure. This is compatible with our previous observations *in vitro* demonstrating that small doses of rotenone stimulated mitophagy in primary cortical neurons without CL oxidation [58]. However, at higher doses, rotenone caused CL oxidation and activation of the apoptotic cell death pathway. It is tempting to speculate that at the early time point, the mitophageal pathway was activated in SN neurons as a rescue mechanism which transitioned to triggering the apoptotic death as the damage was enhanced by increasing doses of rotenone at later time points.

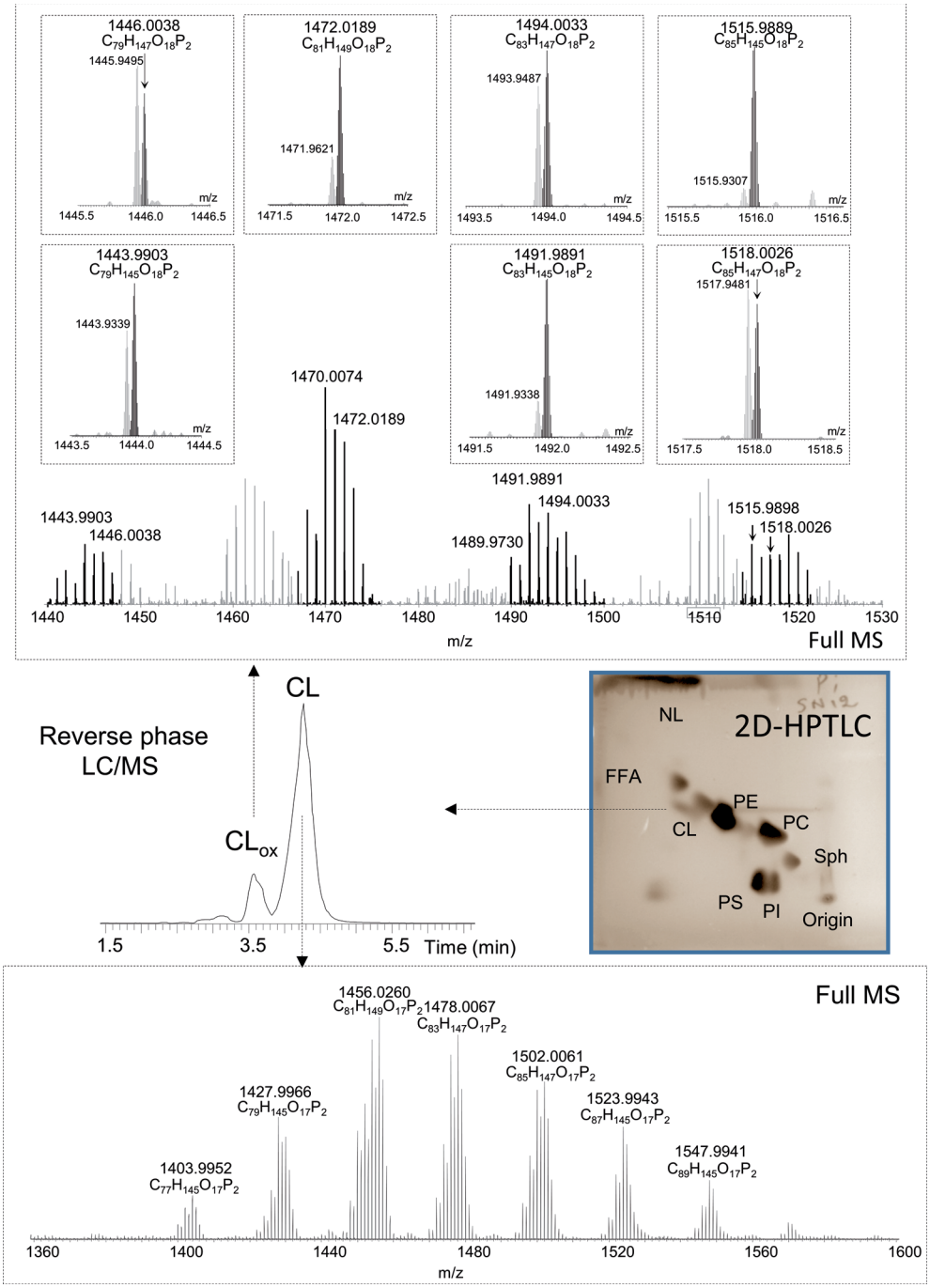

Figure 5. Detection and identification of CL oxygenated species in rat SN. Typical HPTLC of total lipids, LC/MS profile, and mass spectra of CL and its oxygenated species obtained from SN of rat exposed to rotenone (parkinsonian endpoint). CL was isolated by 2D-HPTLC. The CL fraction was then subjected to reverse-phase LC/MS analysis using a C8 column (4.6 mm × 15 cm). CL and oxygenated CL were separated using an isocratic solvent system (see "Methods" section). Under these conditions, oxygenated CL eluted prior to CL. Molecular species of oxygenated CL were identified as mono-oxygenated species based on exact m/z ratios. CL: cardiolipin, FFA: free fatty acids, NL: neutral lipids, PA: phosphatidic acid, PC: phosphatidylcholine, PE: phosphatidylethanolamine, PG: phosphatidylglycerol, PI: phosphatidylinositol, PS: phosphatidylserine, SM: sphingomyelin.

Analysis of CL oxidation products in SN revealed unusual features of rotenone-associated oxidation: (i) exclusive accumulation of oxygenated $C_{18:2}$ in *sn*-1 rather than *sn*-2 position and (ii) selective generation of mono-oxygenated CL species. In line with this, our previous studies identified $C_{18:2}$, located in *sn*-1 position of CL, as the major oxidation substrate in rotenone-treated lymphocytes [20]. Notably, mono-oxygenated CL species were the major products detected in rotenone-exposed lymphocytes [20]. While the mechanisms of this unusual specificity toward $C_{18:2}$ species of CLs remain to be elucidated, they are indicative of enzymatic rather than random stochastic free radical oxidation pathways. One of the candidate catalysts in oxidation of CL is cytochrome c with its established role during apoptosis [15]. Oxidizing equivalents ($O_2\bullet$- –> H_2O_2) formed in mitochondria during apoptosis feed

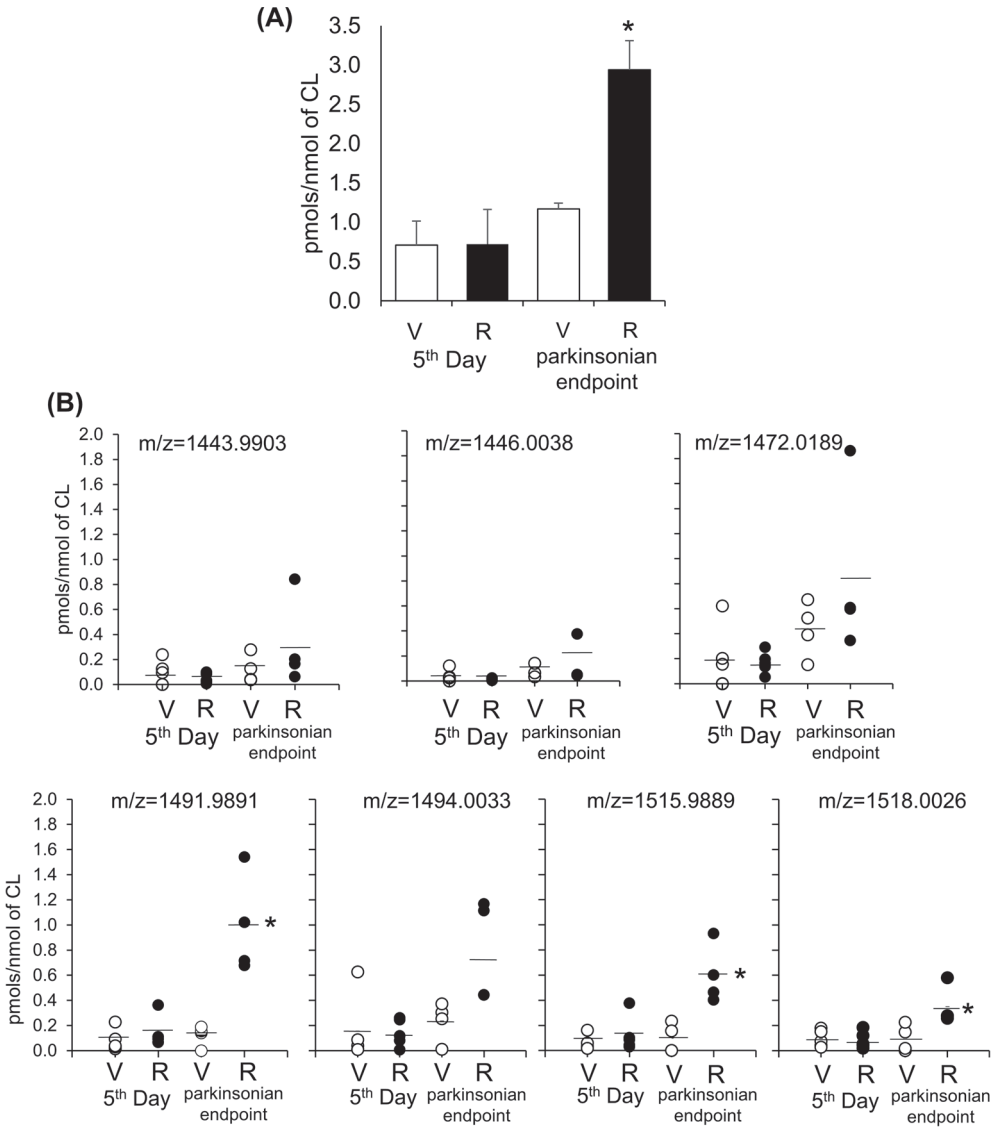

Figure 6. Quantitative assessment of total (A) and individual oxygenated molecular species of CL (B) in SN of control and rotenone-treated rats. V-vehicle; R-rotenone. Molecular species with m/z 1443.9903, 1446.0038, 1472.0189, 1491.9891, 1494.0033, 1515.9889, and 1518.0026 originated from molecular species with m/z 1427.9966, 1430.0077, 1456.0260, 1475.9943, 1478.0067, 1499.9929, and 1502.0061, respectively, after addition of one oxygen. Data are mean ± SD, $n = 4$–5. *$p < 0.05$ versus respective control (vehicle).

the peroxidase activity of cytochrome c/CL complexes resulting in the *selective* depletion of oxidizable CL species in mitochondria and the accumulation of oxygenated CLs [15]. Alternatively, 12/15-lipoxygenase driven mechanisms may be enacted in damaged mitochondria to cause CL oxidation [59]. In the latter case, however, the selectivity to phospholipid substrates (CLs) should be less pronounced. Following oxidation, the hydrolysis reactions—possibly catalyzed by phospholipase A_2—can be involved in depletion of oxidizable CL species in SN of rotenone-treated rats. Recently, we discovered a new biosynthetic pathway for lipid mediators activated *in vivo* after acute tissue injury realized by oxidation and hydrolysis of oxygenated CL species by mitochondrial Ca^{2+}-independent $iPLA_2\gamma$ [18]. Several reports indicate that $iPLA_2$-VI, a calcium-independent PLA_2, may be implicated in the pathogenesis of PD [60–62]. Mutation of PLA2G6, encoding calcium-independent PLA_2, is characteristic of PD and results in the suppression of the enzymatic activity [60]. There are only few publications on the effect of rotenone on $iPLA_2$ activity in mitochondria. In studies on isolated lung and liver mitochondria, rotenone treatment caused the release of PUFA which was partially sensitive to 6E-(bromoethylene)tetrahydro-3R-(1-naphthalenyl)-2H-pyran-2-one, (R)-bromoenol lactone ((R)-BEL) [63,64]. Our in vivo studies, however, did not document higher levels of free fatty acids or oxygenated free fatty acids in SN of rotenone-treated rats versus control rats. Accordingly, with the exception of lysophosphatidylcholine, no accumulation of other lysophospholipids have been observed.

While apoptosis-driven CL oxidation may be accountable for the observed accumulation of oxidized CL, it is likely that non-apoptotic cell death pathways are also triggered in rotenone-treated animals resulting in the release of damaged mitochondria. This may explain the detected higher levels of PUFA CL species in plasma. Indeed, execution of necrop-

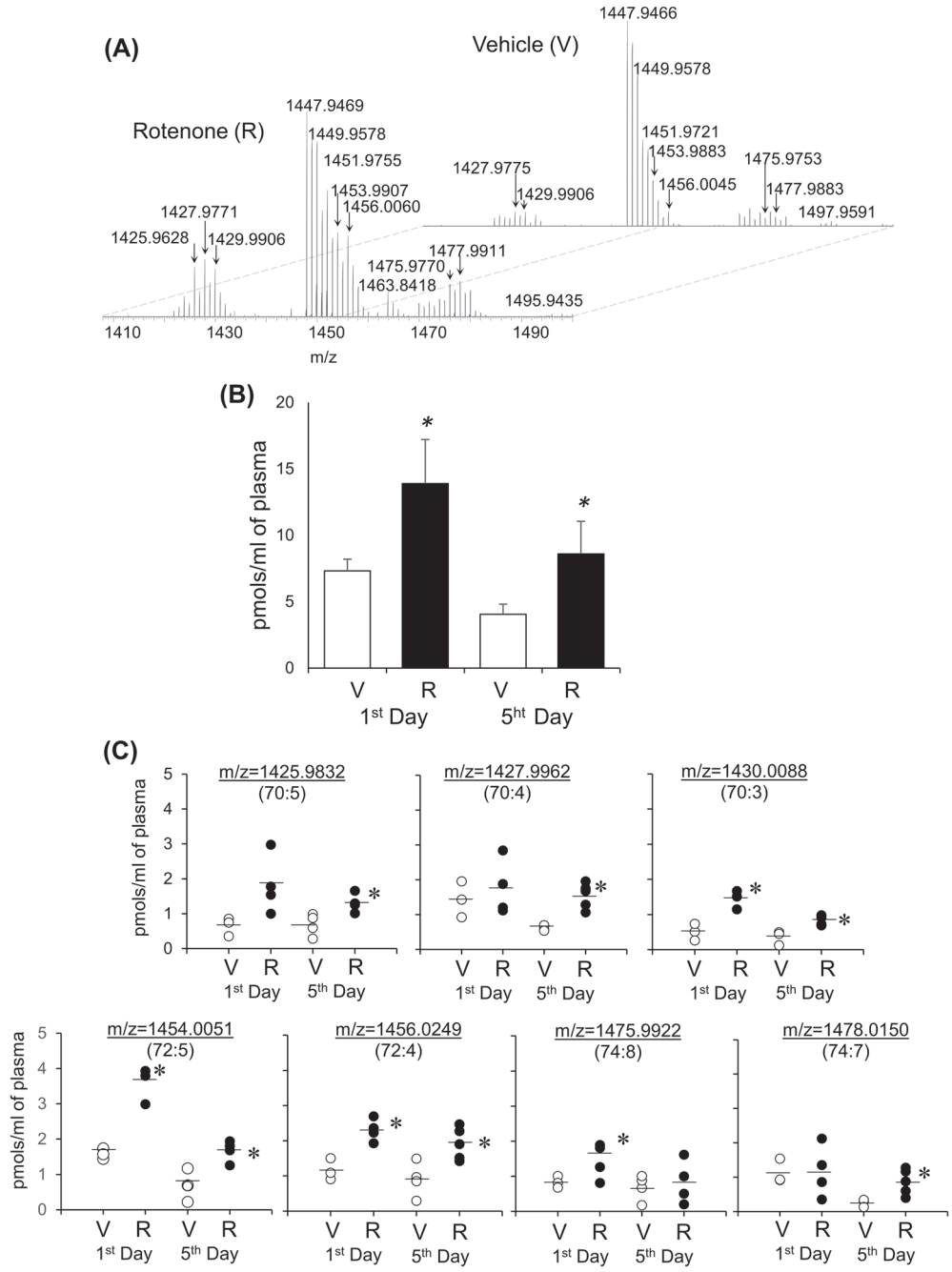

Figure 7. Detection, identification, and quantification of CL in rat plasma. Plasma lipids were separated by normal-phase LC and detected using orbitrap Q-Exactive. A. Typical mass spectra of CL obtained from control rats and rats exposed to rotenone. Quantitative assessment of CL (B) and its individual molecular species (C) in rat plasma. V-vehicle; R-rotenone. Data are mean ± SD, $n = 3–5$. *$p < 0.05$ versus respective control (vehicle). Mass spectra of CL were acquired using a Q-Exactive orbitrap mass spectrometer. Thus, m/z values for CL species were presented to 4 decimal places. Arrows indicate the CL species that accumulated in plasma.

totic program has been shown to trigger release of mitochondria into extracellular compartments [65].

In conclusion, we demonstrated that exposure of rats to rotenone causes depletion of PUFA CL and accumulation of mono-oxygenated CL species in SN and the emergence of elevated levels of CL in plasma. These metabolic CL changes could reflect rotenone-induced mitochondrial dysfunction including mitophageal response at the early time points and enzymatic CL oxidation during execution of programmed cell death pathways (apoptosis and necroptosis) at the later stages after the exposure. Characterization of oxidatively modified CL molecular species in SN and detection of PUFA-containing CL species in plasma may contribute to better understanding of the PD pathogenesis and lead to the development of new biomarkers of mitochondrial dysfunction associated with this disease.

Acknowledgements

Supported by NIH: ES020693, ES020718, NS076511, NS061817, U19AIO68021, PO1 HL114453, NIOSH OH008282, and HFSP-RGP0013/2014.

Declaration of interest

The authors report no declarations of interest. The authors alone are responsible for the content and writing of the paper.

References

[1] Sanders LH, Greenamyre JT. Oxidative damage to macromolecules in human Parkinson disease and the rotenone model. Free Radic Bio Med 2013;62:111–120.

[2] Yao Z, Wood NW. Cell death pathways in Parkinson's disease: role of mitochondria. Antioxid Redox Signal 2009; 11:2135–2149.

[3] Sherer TB, Greenamyre JT. Oxidative damage in Parkinson's disease. Antioxid Redox Signal 2005;7:627–629.

[4] Mogi M, Harada M, Kondo T, Mizuno Y, Narabayashi H, Riederer P, Nagatsu T. The soluble form of Fas molecule is elevated in parkinsonian brain tissues. Neurosci Lett 1996;220:195–198.

[5] Henchcliffe C, Beal MF. Mitochondrial biology and oxidative stress in Parkinson disease pathogenesis. Nat Clin Pract Neurol 2008;4:600–609.

[6] Dias V, Junn E, Mouradian MM. The role of oxidative stress in Parkinson's disease. J Parkinson's Dis 2013;3:461–491.

[7] Schapira AH, Cooper JM, Dexter D, Clark JB, Jenner P, Marsden CD. Mitochondrial complex I deficiency in Parkinson's disease. J Neurochem 1990;54:823–827.

[8] Sofic E, Lange KW, Jellinger K, Riederer P. Reduced and oxidized glutathione in the substantia nigra of patients with Parkinson's disease. Neurosci Lett 1992;142:128–130.

[9] Good PF, Hsu A, Werner P, Perl DP, Olanow CW. Protein nitration in Parkinson's disease. J Neuropathol Exp Neurol 1998;57:338–342.

[10] Alam ZI, Jenner A, Daniel SE, Lees AJ, Cairns N, Marsden CD, et al. Oxidative DNA damage in the parkinsonian brain: an apparent selective increase in 8-hydroxyguanine levels in substantia nigra. J Neurochem 1997;69:1196–1203.

[11] Dexter DT, Carter CJ, Wells FR, Javoy-Agid F, Agid Y, Lees A, et al. Basal lipid peroxidation in substantia nigra is increased in Parkinson's disease. J Neurochem 1989;52:381–389.

[12] Kagan VE. Lipid Peroxidation in Biomembranes. Boca Raton, Florida: CRC Press; 1988.

[13] Yoritaka A, Hattori N, Uchida K, Tanaka M, Stadtman ER, Mizuno Y. Immunohistochemical detection of 4-hydroxynonenal protein adducts in Parkinson disease. Proc Natl Acad Sci USA 1996;93:2696–2701.

[14] Jomova K, Vondrakova D, Lawson M, Valko M. Metals, oxidative stress and neurodegenerative disorders. Mol Cell Biochem 2010;345:91–104.

[15] Kagan VE, Tyurin VA, Jiang J, Tyurina YY, Ritov VB, Amoscato AA, et al. Cytochrome c acts as a cardiolipin oxygenase required for release of proapoptotic factors. Nat Chem Biol 2005;1:223–232.

[16] Kagan VE, Chu CT, Tyurina YY, Cheikhi A, Bayir H. Cardiolipin asymmetry, oxidation and signaling. Chem Phys Lipids 2014;179:64–69.

[17] Tyurina YY, Domingues RM, Tyurin VA, Maciel E, Domingues P, Amoscato AA, et al. Characterization of cardiolipins and their oxidation products by LC-MS analysis. Chem Phys Lipids 2014;179:3–10.

[18] Tyurina YY, Poloyac SM, Tyurin VA, Kapralov AA, Jiang J, Anthonymuthu TS, et al. A mitochondrial pathway for biosynthesis of lipid mediators. Nat Chem 2014;6:542–552.

[19] Samhan-Arias AK, Ji J, Demidova OM, Sparvero LJ, Feng W, Tyurin V, et al. Oxidized phospholipids as biomarkers of tissue and cell damage with a focus on cardiolipin. Biochim Biophysica Acta 2012;1818:2413–2423.

[20] Tyurina YY, Winnica DE, Kapralova VI, Kapralov AA, Tyurin VA, Kagan VE. LC/MS characterization of rotenone induced cardiolipin oxidation in human lymphocytes: implications for mitochondrial dysfunction associated with Parkinson's disease. Mol Nutrition Food Res 2013;57:1410–1422.

[21] Panov A, Dikalov S, Shalbuyeva N, Taylor G, Sherer T, Greenamyre T. Rotenone model of Parkinson disease: multiple brain mitochondria dysfunctions after short term systemic rotenone intoxication. J Biol Chem 2005;280:42026–42035.

[22] Sanders LH, McCoy J, Hu X, Mastroberardino PG, Dickinson BC, Chang CJ, et al. Mitochondrial DNA damage: molecular marker of vulnerable nigral neurons in Parkinson's disease. Neurobiol Dis 2014;70:214–223.

[23] Sanders LH, Howlett EH, McCoy J, Greenamyre JT. Mitochondrial DNA damage as a peripheral biomarker for mitochondrial toxin exposure in rats. Toxicol Sci 2014;142: 395–402.

[24] Martinez TN, Greenamyre JT. Toxin models of mitochondrial dysfunction in Parkinson's disease. Antioxid Redox Signal 2012;16:920–934.

[25] Greenamyre JT, Cannon JR, Drolet R, Mastroberardino PG. Lessons from the rotenone model of Parkinson's disease. Trends Pharmacol Sci 2010;31:141–142.

[26] Folch J, Lees M, Sloane Stanley GH. A simple method for the isolation and purification of total lipides from animal tissues. J Biol Chem 1957;226:497–509.

[27] Bligh EG, Dyer WJ. A rapid method of total lipid extraction and purification. Can J Biochem Physiol 1959;37:911–917.

[28] Boettcher C, Pries C, Vangent CM. A rapid and sensitive sub-micro phosphorus determination. Anal Chim Acta 1961; 24:203.

[29] Tyurina YY, Tyurin VA, Kapralova VI, Wasserloos K, Mosher M, Epperly MW, et al. Oxidative lipidomics of gamma-radiation-induced lung injury: mass spectrometric characterization of cardiolipin and phosphatidylserine peroxidation. Radiat Res 2011;175:610–621.

[30] Rouser G, Fkeischer S, Yamamoto A. Two dimensional then layer chromatographic separation of polar lipids and determination of phospholipids by phosphorus analysis of spots. Lipids 1970;5:494–496.

[31] Sparagna GC, Johnson CA, McCune SA, Moore RL, Murphy RC. Quantitation of cardiolipin molecular species in spontaneously hypertensive heart failure rats using electrospray ionization mass spectrometry. J Lipid Res 2005; 46:1196–1204.

[32] Bove J, Prou D, Perier C, Przedborski S. Toxin-induced models of Parkinson's disease. NeuroRx 2005;2:484–494.

[33] Betarbet R, Sherer TB, Greenamyre JT. Animal models of Parkinson's disease. BioEssays 2002;24:308–318.

[34] Greenamyre JT, Sherer TB, Betarbet R, Panov AV. Complex I and Parkinson's disease. IUBMB Life 2001;52:135–141.

[35] Testa CM, Sherer TB, Greenamyre JT. Rotenone induces oxidative stress and dopaminergic neuron damage in organotypic substantia nigra cultures. Brain Res Mol Brain Res 2005; 134:109–118.

[36] Krysko DV, Agostinis P, Krysko O, Garg AD, Bachert C, Lambrecht BN, et al. Emerging role of damage-associated molecular patterns derived from mitochondria in inflammation. Trends Immunol 2011;32:157–164.

[37] Aldrovandi M, O'Donnell VB. Oxidized PLs and vascular inflammation. Curr Atheroscler Rep 2013;15:323.

[38] Bochkov VN, Oskolkova OV, Birukov KG, Levonen AL, Binder CJ, Stockl J. Generation and biological activities of oxidized phospholipids. Antioxid Redox Signal 2010;12: 1009–1059.

[39] Ashraf MZ, Kar NS, Podrez EA. Oxidized phospholipids: biomarker for cardiovascular diseases. Int J Biochem Cell Biol 2009;41:1241–1244.

[40] Schlame M, Ren M. The role of cardiolipin in the structural organization of mitochondrial membranes. Biochim Biophys Acta 2009;1788:2080–2083.

[41] Daum G, Lees ND, Bard M, Dickson R. Biochemistry, cell biology and molecular biology of lipids of Saccharomyces cerevisiae. Yeast 1998;14:1471–1510.
[42] Fry M, Green DE. Cardiolipin requirement for electron transfer in complex I and III of the mitochondrial respiratory chain. J Biol Chem 1981;256:1874–1880.
[43] Sharpley MS, Shannon RJ, Draghi F, Hirst J. Interactions between phospholipids and NADH:ubiquinone oxidoreductase (complex I) from bovine mitochondria. Biochemistry 2006;45:241–248.
[44] Robinson NC. Functional binding of cardiolipin to cytochrome c oxidase. J Bioenerg Biomembr 1993;25:153–163.
[45] Eble KS, Coleman WB, Hantgan RR, Cunningham CC. Tightly associated cardiolipin in the bovine heart mitochondrial ATP synthase as analyzed by 31P nuclear magnetic resonance spectroscopy. J Biol Chem 1990;265:19434–19440.
[46] Bayir H, Tyurin VA, Tyurina YY, Viner R, Ritov V, Amoscato AA, et al. Selective early cardiolipin peroxidation after traumatic brain injury: an oxidative lipidomics analysis. Annals Neurol 2007;62:154–169.
[47] Ji J, Kline AE, Amoscato A, Samhan-Arias AK, Sparvero LJ, Tyurin VA, et al. Lipidomics identifies cardiolipin oxidation as a mitochondrial target for redox therapy of brain injury. Nature Neuroscience 2012;15:1407–1413.
[48] Tyurina YY, Tyurin VA, Kaynar AM, Kapralova VI, Wasserloos K, Li J, et al. Oxidative lipidomics of hyperoxic acute lung injury: mass spectrometric characterization of cardiolipin and phosphatidylserine peroxidation. Am J Physiol Lung Cell Mol Physiol 2010;299:L73–85.
[49] Tyurina YY, Kisin ER, Murray A, Tyurin VA, Kapralova VI, Sparvero LJ, et al. Global phospholipidomics analysis reveals selective pulmonary peroxidation profiles upon inhalation of single-walled carbon nanotubes. ACS Nano 2011;5: 7342–7353.
[50] Tyurina YY, Tyurin VA, Epperly MW, Greenberger JS, Kagan VE. Oxidative lipidomics of gamma-irradiation-induced intestinal injury. Free Radic Biology Med 2008;44:299–314.
[51] Kiebish MA, Han X, Seyfried TN. Examination of the brain mitochondrial lipidome using shotgun lipidomics. Methods Mol Biol 2009;579:3–18.
[52] Murphy MP. How mitochondria produce reactive oxygen species. Biochemical J 2009;417:1–13.
[53] Paradies G, Paradies V, De Benedictis V, Ruggiero FM, Petrosillo G. Functional role of cardiolipin in mitochondrial bioenergetics. Biochim Biophysica Acta 2014;1837: 408–417.
[54] Bogdanov M, Mileykovskaya E, Dowhan W. Lipids in the assembly of membrane proteins and organization of protein supercomplexes: implications for lipid-linked disorders. Subcell Biochem 2008;49:197–239.
[55] Celardo I, Martins LM, Gandhi S. Unravelling mitochondrial pathways to Parkinson's disease. Br J Pharmacol 2014;171:1943–1957.
[56] Palikaras K, Tavernarakis N. Mitophagy in neurodegeneration and aging. Front Genet 2012;3:297.
[57] Radi E, Formichi P, Battisti C, Federico A. Apoptosis and oxidative stress in neurodegenerative diseases. J Alzheimer's Dis 2014;42:S125–152.
[58] Chu CT, Ji J, Dagda RK, Jiang JF, Tyurina YY, Kapralov AA, et al. Cardiolipin externalization to the outer mitochondrial membrane acts as an elimination signal for mitophagy in neuronal cells. Nat Cell Biology 2013;15:1197–1205.
[59] Coffa G, Brash AR. A single active site residue directs oxygenation stereospecificity in lipoxygenases: stereocontrol is linked to the position of oxygenation. Proc Natl Acad Sci USA 2004;101:15579–15584.
[60] Morgan NV, Westaway SK, Morton JE, Gregory A, Gissen P, Sonek S, et al. PLA2G6, encoding a phospholipase A2, is mutated in neurodegenerative disorders with high brain iron. Nat Genet 2006;38:752–754.
[61] Lu CS, Lai SC, Wu RM, Weng YH, Huang CL, Chen RS, et al. PLA2G6 mutations in PARK14-linked young-onset parkinsonism and sporadic Parkinson's disease. Am J Med Genet B Neuropsychiatr Genet 2012;159B:183–191.
[62] Kauther KM, Hoft C, Rissling I, Oertel WH, Moller JC. The PLA2G6 gene in early-onset Parkinson's disease. Mov Disord 2011;26:2415–2417.
[63] Jaburek M, Jezek J, Zelenka J, Jezek P. Antioxidant activity by a synergy of redox-sensitive mitochondrial phospholipase A2 and uncoupling protein-2 in lung and spleen. Int J Biochem Cell Biol 2013;45:816–825.
[64] Rauckhorst AJ, Broekemeier KM, Pfeiffer DR. Regulation of the Ca(2+)-independent phospholipase A2 in liver mitochondria by changes in the energetic state. J Lipid Res 2014;55:826–836.
[65] Maeda A, Fadeel B. Mitochondria released by cells undergoing TNF-alpha-induced necroptosis act as danger signals. Cell Death Dis 2014;5:e1312.